Proceedings of the ASME 2017 International Mechanical Engineering Congress and Exposition
IMECE2017
November 3-9, 2017, Tampa, Florida, USA

IMECE2017-72636

VIBRATION ANALYSIS OF HIGH-SPEED END MILLING OPERATIONS APPLIED TO INJECTION MOLD MATERIALS

Andris Logins
PhD student
Department of Material Processing Technology
Riga Technical University,
Riga, Latvia

Toms Torims
Professor
Department of Material Processing Technology
Riga Technical University,
Riga, Latvia

Pedro Rosado Castellano
Professor
Department of Industrial Systems Engineering and Design,
Universitat Jaume I,
Castellón, Spain.

Santiago Gutiérrez
Professor
Department of Mechanical and Materials Engineering
Universitat Politècnica de València, Valencia, Spain

Rafael Torres
Professor
Department of Mechanical and Materials Engineering
Universitat Politècnica de València, Valencia, Spain

ABSTRACT

High-speed milling has often been applied in injection mold manufacturing processes, where surface roughness is a significant criterion in product quality demands. It is equally applicable to automotive or industrial engineering and to toy manufacturing, where plastic parts with a high-quality surface finish have been processed using the injection molding technique. High-speed milling involves a number of process parameters that may affect the 3D surface topography formation. Literature analysis reveals that dynamical behavior is a significant factor in the end milling process on surface roughness parameters. To improve the accuracy of predicted surface topography models, it is important to include the dynamical behavior of milling factor.

This paper describes the surface prediction model of combined end-milling geometrical and dynamical interaction models. The natural frequency of machine assembly and forced vibrations during the cutting process were measured during the flat-end milling process. Unevenly distributed cutting marks were revealed by surface 3D topography images and microscopy images of the machined samples.

A mathematical model to predict surface topography was developed, including dynamical behavior and cutting geometries. Machine accuracy also has to be addressed. 3D surface topography parameters from the experimental sample provided the results for the mathematical prediction model. This model offers a software tool for manufacturers to improve the quality of machined part surfaces, taking into account the behavioral properties of their machining equipment. Relevant conclusions about the manufacturing equipment accuracy have been drawn. Vibrations in the milling system affect the cutting process and contribute to the surface topography prediction model. Local cutting tool vibrations do not have any influence on surface parameter mean values.

INTRODUCTION

A well-developed surface topography prediction model should be based on theoretical knowledge of the cutting process. Conventional, low-speed cutting processes have been modeled by various authors for more than half a century [1-3]. Even so, a High Speed Machining (HSM) process model that

can describe the machined surface still encounters difficulties and inaccuracies. Most of them are related to a failure to include the most important cutting parameters [4-6].

In this field there have been a number of empirically based research projects, where authors try to eliminate the impact of model accuracy errors in their developed models. Due to the changes in machining environment (machine manufacturer, tool chuck, tool manufacturer and material), the model accuracy is highly variable. Sometimes, these models are not at all applicable for other types of milling machines, due to other factors influencing the milling processes.

The revolve axis in end-mill operations suffers from deviations compared with the theoretical model, which affects the final tool trajectory. This new trajectory is created by deformations of the cutting tool due to tool deflection, constantly variable cutting forces, constant or variable tool-axis inclination or machine head/spindle alignment inaccuracy. Due to constant cutting tool-axis inclination error, tool mounting errors etc., maximum height in the scale-limited surface area parameter depends on the machining direction. Analyzing opposite machining directions may reveal this phenomenon.

Until now, a number of authors have developed their mathematical models based on the milling tool radial run-out effect [2, 3, 12]. This is one of the most important geometrical parameters acting on the cutting process that influences the surface roughness formation. Radial run-out results in irregular uncut chip thickness and cutting forces, respectively. This generates vibration during the cutting process.

At this stage of the research, the main goal is to determine mathematically the influence of machine-tool-workpiece system inaccuracies and properties on a real surface height parameter S_z. Dynamical (vibration) effect, tool deflection and alignment, a combination of tool geometry and sharpening inaccuracy (relative to the plane of the tool path) are the parameters under review. This article provides improved analysis of the previously developed tool deflection model and compares predicted results with measured surface topography parameter S_z values. The model has been enhanced by including the vibrational behavior of the machining system.

NOMENCLATURE

α	tool tip point concavity angle
a_p	cutting depth
θ	milling head inclination angle
λ	tool immersion angle measured by the Y axis
$\delta X, \delta Y, \delta Z$	cutting tip point displacement in the X, Y and Z dir.
δz_{vib}	maximum vibration amplitude in the Z axis direction
f	*c*utting feed
f_m	mark repeating frequency
f_t	*t*ool deflection frequency
F_n, F_t, F_a	normal, tangential and axial forces
n	*s*pindle speed
R_a	arithmetic mean roughness
R	circle length of the tool tip point
S_a	*a*rithmetic mean surface height
S_{ku}	kurtosis of the scale-limited surface
S_q	root mean square height of the scale-limited surface
S_z	maximum height of the scale limited surface
T	tool rotation frequency period
t	*t*ime
V_c	*c*utting speed
θ_T	milling head inclination angle

STATE OF THE ART

A number of authors have considered cutting geometry to justify surface 2D roughness parameters. In the 1980s, authors such as T.S. Babin et al. [1] were among the first to start a comprehensive research programme to analyze the influence of machining process parameters on surface roughness formation in the end milling process. These authors considered both cutter run-out and tool deflection error, and their influence on basic tool path equations. They developed an analytical model which describes the cutting edge trajectory and its influence on the machined surface profile height. Sutherland et al. considered two types of run-out involved in the process: parallel axis radial run-out and axis tilt run-out [2], [3]. Subsequently, the same model was applied to analyze the influence of cutting regimes on the surface formation of different materials. A similar approach was taken by authors I.B. Corral et al. [4], [5], and M. Arizmedi et al. [6]

A more comprehensive study of cutting dynamics was introduced by Y. Altintas et al. [7] and Budak et al. [8]. The authors analyzed dynamical models of other researchers. A dynamical model with two degrees of freedom is shown in Figure 1.

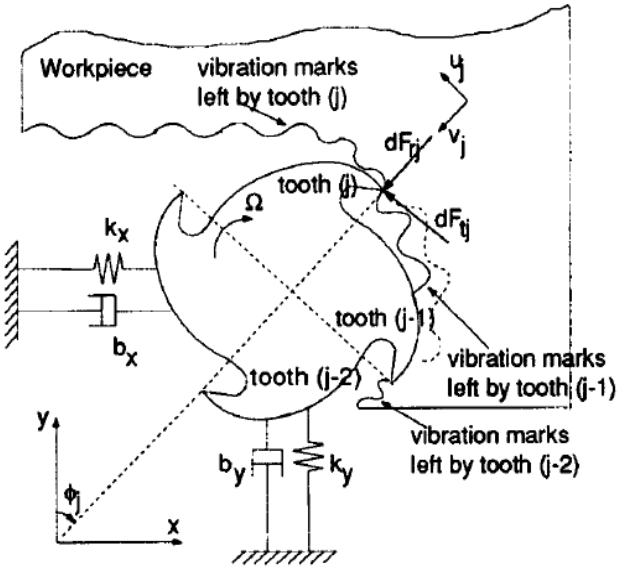

Figure 1. Dynamical model of a cutting system with two degrees of freedom [7]

The dynamics of the system act on the cutting process. The chip load and cutting forces during tool overlap become greater with dynamic behavior. Dynamic tool displacement affects surface formation and cusp height on a laterally machined or ball-end milled surface. [7] Peak distribution is similarly affected on a flat-end machined surface. Furthermore, dynamic cutting forces directly influence tool deflection.

Other authors, such as D. K. Baek et al., have developed a dynamic surface roughness model for face-milling operations. They considered the static and dynamic characteristics of the cutting process. Cutting conditions were combined with specific geometric aspects, including each cutting edge run-out. Relative displacement from forced vibrations in feed direction may affect tool radial run-out error and depth of cut. In the milling process, there are forced and regenerative types of vibrations. Forced vibrations cause instant tool deflection. Regenerative vibrations appear when the cutting system cannot follow the system dynamics due to imposed cutting vibrations. These vibrations should be absolutely avoided, due to their influence on surface roughness. The authors did not consider forced displacement normal to the feed rate. They modeled the milling system with one degree of freedom. [9]

Proposed results of this simple model provide basic conclusions that dynamic cutting model can be applied to predict surface roughness more accurate than analytical models do. Variable feed rate and dynamics of cutting process affect the surface topography more than every other condition based factor. However, authors [9] conclude that run-out values of every particular cutting edge affect surface formation more than the system's dynamic behavior. Nevertheless, these dynamical models are used in most research to investigate the vibration influence on surface roughness. [10]

Weremczuk et al. [11] sought to eliminate the vibrations during the milling process. To analyze the active vibrations, they used the same dynamical system behavior concept as in previous research. They applied dynamical system behavior to both the tool and the workpiece. Two nonlinear differential equations were used for the system calculation, considering different damping and spring coefficients, as well as different mass and opposite force vectors. The difference from previous models is in chip load calculation, where uncut chip thickness was calculated by taking into account the dynamical behavior of both the tool and workpiece. [11]

The latest model, which includes the most important kinematic-geometrical factors, was proposed by Wojciechowski et al. [12] In their research they combine the influence of cutting parameters, tool static radial run out and deflections induced by cutting forces, to develop a versatile surface roughness model for the cylindrical milling of the laterally machined surface. This model is presented as a reliable model to predict surface R_a and R_z values. Tool displacement combined with radial run-out and dynamical displacement provides a reasonable result, but the authors mention a discrepancy value of up to 20% for the Ra parameter and up to 39% for the R_z parameter. They also indicate that simultaneous impact of tool radial run-out and tool dynamical deflection greatly affects the surface roughness.

As it is possible to see from this research, most authors have only looked at conventional 2D surface roughness models, but more complete information can be obtained from a 3D surface topography model.

The main goal of this research is to combine these dynamical effects and static tool geometry to obtain a 3D surface model for an end-mill machined flat surface. This research considers static and dynamical behavior of milling process and its influence on surface 3D topography parameters. The flat-end milling procedure is performed to analyze the impact of cutting dynamics on surface topography.

METHODOLOGY

This research forms part of more comprehensive research started by the same authors. Previous investigation considered how cutting parameters influence 3D surface topography parameters. Irregular cutting marks were observed on the surface. This time, other, more important process parameters such as vibrations from the cutting process will be included. To support the aforementioned statements and understand the cause of the variable distances between feed rate marks in previous samples [13], it is necessary to conduct an experiment and measure the milling machine vibrations at initial and working stages. The combination of process dynamics and geometry will provide more extensive knowledge about surface formation in high-speed milling processes.

The experiments and measurements were repeated in the same way as previously, using the same materials, tool type and sample types. Two Mitsubishi TiAlN-coated flute cylindrical-end milling tools MS2MSD1000 were used. The cutting process was performed under the following cutting conditions:

a) Feed: f = 0.1 mm/tooth

b) Spindle speed: n = 4775 rpm, equivalent to cutting speed v_c = 150 mm/min

c) Cutting depth: a_p = 0.3mm

The tool path followed the perimeter of a rectangular zone. A total of four straight tool movements (each side of the rectangle) were made using the Up milling mode. Straight tool movement in every feed direction was monitored. The cutting areas in the sample are represented in Figure 2. Following the cutting direction, four measuring points were selected: 1. = South, 2. = West, 3. = North and 4. = East.

The material selected for machining was C45/ AISI 1045 carbon steel. This material is widely used for injection mould production, where the obtained surface topography is of significant importance for the final product quality.

A Kondia B500 milling machine was used. A Mitsubishi flat-end milling tool MS2MSD1000 with a cutting diameter (D) of 10mm was used for cutting. Samples were prepared at the Universitat Politècnica de València, in Spain.

The 3D surface topography measurements were taken with a Bruker Contour GT3 optical measuring device. All the measuring was done at Tallinn University of Technology, in the Faculty of Mechanical Engineering. The measured data files were processed with an in-house analytical software tool. This tool and the software calculations are based on the ISO 25178-2:2012 Geometrical Product Specification standard. [14] The in-house software is based on the Python programming language. Furthermore, the surface topography was photographed to make analysis more comprehensive.

In addition, vibration measurements of the milling spindle have been considered during the cutting process. Vibrations

were measured with accelerometers, attached to the machine table and spindle.

In Figure 2, the machining strategy and measuring order of experimental samples are illustrated.

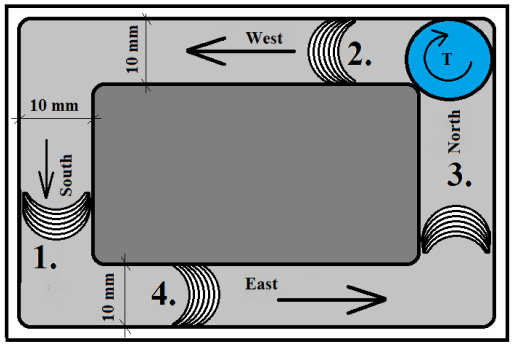

Figure 2. Machining strategy for sample with rectangular cutting tool movement

The following cutting conditions were used to prepare the samples:

Table 1. Experimental design

Conditions	Samples Nº.		
	2. and 6.	1. 3. 5. and 7.	4. and 8.
Feed rate, mm/tooth	0.04	0.1	0.2
Feed speed, mm/min	382	954.9	1909.9
Overlap, mm	2.5/5/10	2.5/5/10	2.5/5/10
Cutting mode,	Up	Up	Up
Machine	Kondia B500	Kondia B500	Kondia B500
	Gentiger GT-66V-T16B	Gentiger GT-66V-T16B	Gentiger GT-66V-T16B
Tool length, mm	34.8 mm	34.8 mm	34.8 mm

For the experiment, 8 different samples were prepared. Every sample was machined under different conditions, including ¼, ½ tool overlapping and without overlapping.

To analyze the vibrations in the machine-tool-workpiece system, the natural frequency measurements of the machining center were also taken. Figure 3 presents a diagram of the measurements. To measure the milling machine vibrations, an accelerometer was attached to the workpiece and the spindle. Vibration measurements were recorded at every working stage, including the machine's initial state. Initial state measurements allow us to isolate certain external vibrations, which are unrelated to machine errors or cutting process errors.

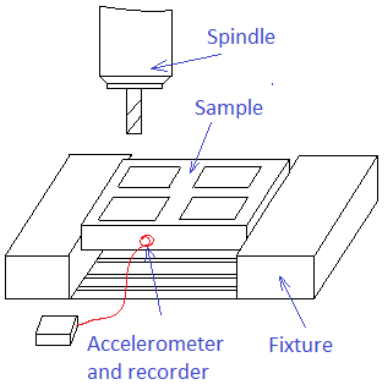

Figure 3. Schematic representation of cutting process vibration experimental measurements

RESULTS

Literature analysis offers some conclusions about the most significant cutting process parameters involved in High Speed Machining. One of the factors that cannot be neglected is the vibration effect of the cutting system and the tool's natural vibration frequency, the tool-chuck interface and the milling machine as itself. A great deal of analysis has been conducted on the behavior of milling process vibrations and dynamics, and their influence on laterally machined surface roughness parameters, or on cutting force. [8, 10-12] To complete the mathematical model so that it includes the influence of the flat-end cutting parameter, the dynamical cutting process has to be incorporated.

Analysis of the natural tool frequency was achieved in two ways.

-Firstly: FEM analysis

FEM analysis was performed for a realistic CAD model of the cutting tool, with the same tool length as the one used in the experiments, in order to analyze the natural vibration frequencies. Analysis shows different deformation modes related to the natural frequency of the cutting tool geometry and material type.

A 10 mm flat-end milling tool CAD model was developed for the Mitsubishi Tungsten carbide milling tool. Table 2. presents the FEM simulation results for the flat-end milling tool natural frequency for the first two deformation modes – axial deflection. In Figure 4. tool deflection amplitude (amplified) can be seen due to the force acting on the tool tip point.

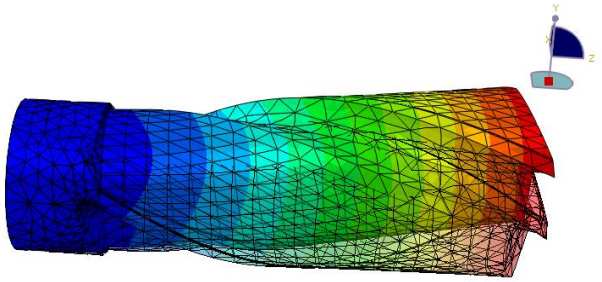

Figure 4. Flat-end mill axial deflection

Table 2. Natural frequency simulation results

Index	Increment	Type	Cycles/second (Hz)
1	MODE 1	Axial Deflection	6907.7
2	MODE 2	Axial Deflection	7590.7
3	MODE 3	Torsional Deformation	30024
4	MODE 4	Axial Deflection 2 DoF	34831
5	MODE 5	Axial Deflection 2 DoF	38046
6	MODE 6	Extensional Deformation	47654
7	MODE 7	Axial Deflection 3 DoF	81370
8	MODE 8	Axial Deflection 3 DoF	85480
9	MODE 9	Torsional deformation 2 DoF	88876

The deformation modes refer to the different types of deformations introduced by the natural vibration frequency. The first and second mode, in Table 2, represent tool axial deflection along the rotational axis, where all the other tool degrees of freedom (DoF) are restricted in one point, fixed into the tool chuck. The third mode describes tool torsional deformation with the same conditions as previously. Modes 4 and 5 represent tool deflection along the orthogonal planes, when one more degree of freedom is restricted perpendicular to the deflection plane. Mode 6 represents tool extension deformation, with only one point of tool fixation, the tool chuck. Modes 7 and 8 represent tool deflection along the orthogonal planes, similar to modes 1, 2, 4 and 5, but one more degree of freedom is restricted at two tool points. Mode 9 represents tool torsional deformation around the tool's rotational axis, with one more fixed degree of freedom.

The other modes generated by the application are basically not representative, as they repeat the same behavior, except that the restricted degrees of freedom are located in multiple points.

As can be seen from the cutting tool FEM analysis, the frequency for the 1st and 2nd types of natural frequency modes is similar due to deflection deformation along the orthogonal planes. It depends solely on tool geometry. Due to the units used for material properties and model dimensions, the simulated frequency units are in *Hz*.

Figure 5. shows marks on the material's surface, left from tool vibrations during the machining process. These marks seem to be a local deformation of the surface height, caused by tool deformations due to natural frequency vibrations. If we look carefully, we can see that this behavior is repeated in every sample, at any feed speed.

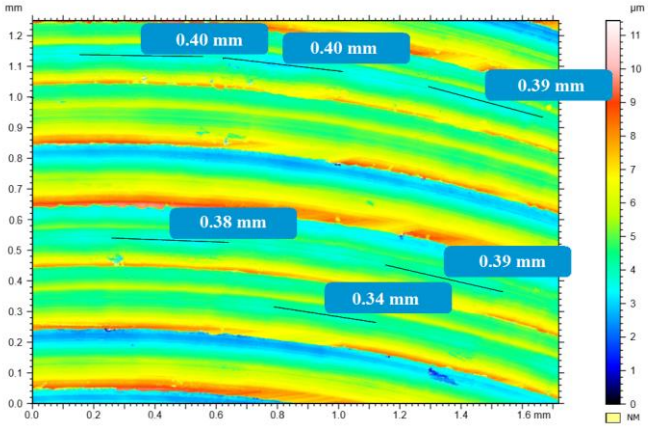

Figure 5. Marks left from the tool's natural frequency vibration

The frequency calculated for the repeating marks in Figure 5 is similar to the natural frequency of the first and second FEM analysis modes.

The distance between the marks is 0.36 – 0.4 mm, where the Spindle rotation frequency is 4775 rpm. Therefore, the tool rotation frequency period is:

$$T = 60/4775 = 0{,}012 \text{ sec/rev}, \quad (1)$$

Tool tip radius, R = 5mm:

$$C = 3{,}14 \times R \times 2 = 31{,}4159 \text{ mm} \quad (2)$$

The mark repetition frequency for one tool revolution:

$$f_m = 31{,}4159 / 0{,}36 = 87.27 \text{ times} \quad (3)$$

$$f_t = 87.27/0{,}012 = 7272{,}21 \text{ Hz (times per second)} \quad (4)$$

The frequency of these marks is similar to the natural frequency of the first two deformation modes – 6907 and 7590 Hz, respectively. The authors suspect that these marks are left due to the natural frequency vibrations of the cutting tool. The height of these marks change with this frequency.

-Secondly: Frequency analysis

The measurements of machine-tool-workpiece system natural frequency were taken on the machine. The fast response function (FRF) was used to calculate the natural frequency of milling machines. FRF is the system's output spectrum response function and is measured in $m/s^2/N$. The results are shown in Figure 6. It provides information about the table natural frequency on the machine's X and Y axes. In this case,

applying auxiliary force with a hammer on the machine table and spindle, the measured natural frequency of the machine milling table was:

X direction – 76 Hz,
Y direction – 78 Hz.

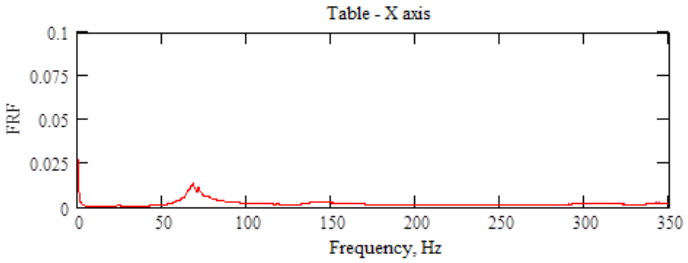

Figure 6. Fast response function (FRF) analysis of the Kondia CNC milling machine spindle X axis

Visual analysis of the machined surface 3D topography images, Figure 7 for example, shows the marks with an irregular repeat frequency. Between some marks, the distances are equal to feed. Between other similar marks, this distance increases or decreases in the feed direction.

The same was observed with surface height. A color map of the surface image in Figure 7 represents how surface height varies between the tooth passage marks. This phenomenon can be described as the tool's natural frequency compounded with its axial deflection caused by excitation forces working on the cutting process. The difference varies with the sample cutting direction. Therefore, the influence of this effect also varies due to the cutting forces, as these are also affected by machine alignment inaccuracy.

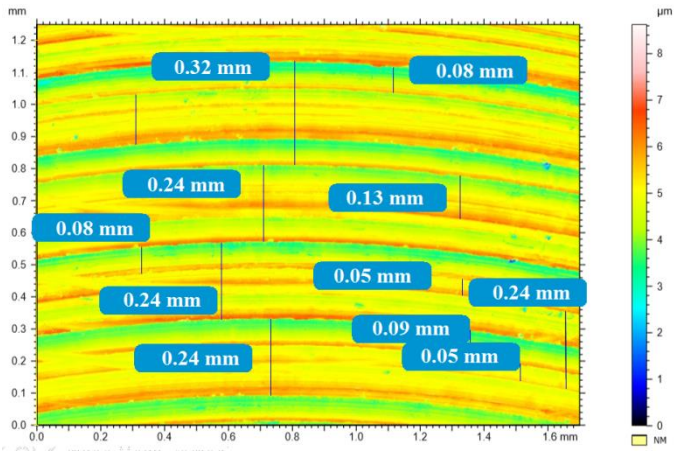

FIGURE 7. Distribution of cutting marks over the material surface after the end milling process

The surface topography height parameter influenced by the tool's forced deflection was calculated previously, considering tangential (F_t), normal (F_n) and axial (F_a) cutting forces against the tool's cutting edge (Figure 8). [14]

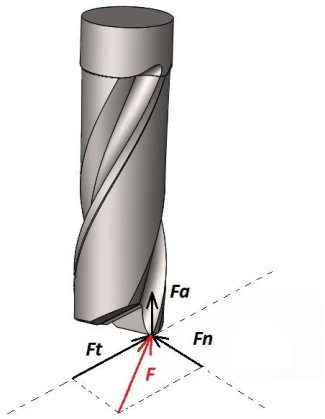

Figure 8. Cutting forces working against a flat-end mill tip point

Data from the tool's cutting-edge displacement due to its natural vibration frequency are collected from the FEM simulation. Data analysis provided tool material stiffness coefficients, see Table 3.

TABLE 3. Material C45 rigidity coefficients

Deformation direction		*Stiffness coefficient, N/mm*
Tangential		M_r = 8146.374
Normal		M_n = 11334.784
Axial	Tangential component	$M_{z(t)}$ = 40150.968
	Normal component	$M_{z(n)}$ = 57703.738
	Axial component	$M_{z(a)}$ = 15885.716

Where M_r –is the cutting tool material rigidity in the normal force direction, M_t is the cutting tool material rigidity in the tangential force direction, $M_{z(t)}$ is the cutting tool material rigidity in the axial direction caused by tangential force influence, $M_{z(n)}$ is the tool rigidity in the axial direction caused by normal force influence and $M_{z(a)}$ is the tool rigidity in the axial direction caused by axial force influence.

The tool deflection model, in accordance with the global machine coordinate system, was calculated by substituting rigidity coefficients into the force model (Eq. 5, 6 and 7).

$$\delta X(Fx(\lambda)) = -Ft(\lambda) * \frac{1}{Mt} * \cos(\lambda) - Fn(\lambda) * \frac{1}{Mn} * \sin(\lambda) \quad (5)$$

$$\delta Y(Fy(\lambda)) = Ft(\lambda) * \frac{1}{Mt} * \sin(\lambda) - Fn(\lambda) * \frac{1}{Mn} * \cos(\lambda) \quad (6)$$

$$\delta Z(F(\lambda)) = \left(-Ft(\lambda) * \frac{1}{Mz(t)}\right) + \left(-Fn(\lambda) * \frac{1}{Mz(n)}\right) + \left(Fa(\lambda) * \frac{1}{Mz(a)}\right) \quad (7)$$

Where λ – is the tool immersion angle measured through the Y axis and F_n, F_t and F_a are the normal, tangential and axial forces respectively.

Total surface height variation in the Z axis direction, $\delta_z(\lambda)$, is calculated as a sum of each calculated component. This model can be improved by including the machine-tool-workpiece system's natural frequency, causing tool tip point displacement in the Z axis (Eq. 8). The sum of these will give a more accurate surface maximum height in the scale-limited surface area parameter Sz. Results are presented in Table 4.

$$\delta z(\lambda) = \delta z_x(\lambda) + \delta z_y(\lambda) + \delta Z\big(F(\lambda)\big) + \delta z_T(\lambda) + \delta z_{vib} \qquad (8)$$

Where $\delta z_x(\lambda)$ and $\delta z_y(\lambda)$ are the tool tip Z height differential from inclination at the X and Y axis respectively and $\delta z_T(\lambda)$ is the total tool tip point differential [14]:

$$\delta z_T(\lambda) = \frac{t(\lambda)*\tan(\theta+\sigma)}{1+\tan(\theta+\sigma)*\tan(\theta)} \qquad (9)$$

Where θ –is the milling head inclination angle without tool deflection angle and σ is the secondary cutting edge radial relief angle.

$\delta z_x(\lambda)$ and $\delta z_y(\lambda)$ – are the machine milling head alignment errors caused by deviations on the X and Y axis respectively [14].

δz_{vib} is the maximum vibration amplitude in the Z axis direction due to machine-tool-workpiece system forced vibrations. This value is obtained by calculating the second order differential equation of the forced vibration system:

$$M \times \left(\frac{d}{dt^2} y(t)\right) + C \times \left(\frac{d}{dt} y(t)\right) + K \times y(t) = f(t) \qquad (10)$$

$$f(t) = Fa(\lambda(t)) * \sin(\lambda(t)) \qquad (11)$$

Where λ(t) is the tool immersion angle, as a function of time. The graph of forced vibrations represents the vibrational amplitude values for the system displacement on the Z axis, and is illustrated in Figure 9.

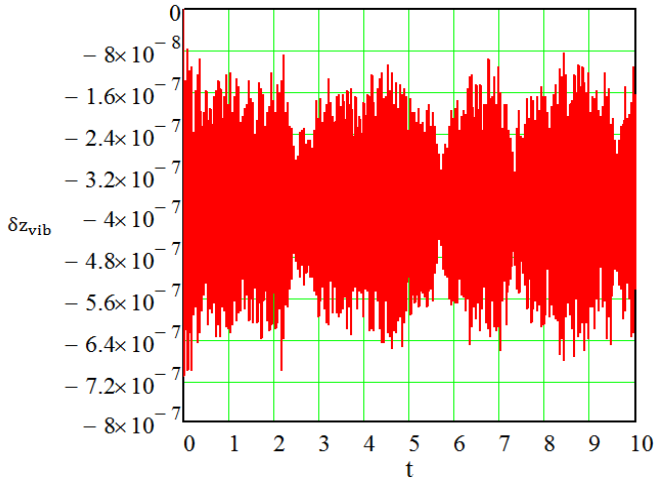

Figure 9. Solved second order vibration system equation

Where δz_{vib} is in millimeters and 't' in seconds.

Predicted values represent the worst scenario due to vibrational influence. If tool inclination, angular displacement and vibration all coincide to cause deflection in one phase, this may result in greater surface roughness.

Table 4. Measured and predicted surface topology parameters analysis

Feed direction	Sa value measured, μm	Sz value measured, μm	Sz value simulated, μm	Difference error between measured and predicted, μm, %	Difference error between directions, %	
					Measured	Predicted
1. South	1.01733	10.60445	9.46012	0.43775 4%	24%	25%
	1.16082	9.19131				
3. North	1.14825	8.0833	7.55194	0. 43898 7%		
	0.89045	7.89854				
2. West	1.12516	8.29217	7.84908	0.59132 5%	16%	18%
	1.16229	8.46029				
4. East	1.00001	9.33774	9.16303	0.52656 5%		
	1.09779	10.04144				

CONCLUSIONS

Taking into account the results described above, the following conclusions can be drawn.

Surface topography images have confirmed the effect of the vibrational behavior of the machine-tool-workpiece system. Differences in distances between cutting marks identified on the material surface topography provide evidence for the vibrational effect of the cutting system. This effect has been introduced into the developed mathematical model to predict the surface height parameter S_z.

The milling tool's local natural frequency has a minor effect on surface topography formation. These vibrations cause some local displacement on the point of the tool tip and may generate local surface parameter S_z changes. They do not have a global effect on the surface parameter S_z, as they do not affect the parameter's mean value.

All the listed effects, including tool alignment error, tool deflection, tool concavity angle and its subsequent minimal surface roughness performed, sharpening errors, etc., provide a result with high prediction accuracy. The mathematically obtained results are compared with the outcome of surface topography measurements using an optical measuring device. Discrepancies between predicted and measured values are less than 10% and the differences between results of tool movement direction do not exceed 2%. This outcome is precise for calculations made for a specific milling system, given the machine milling head alignment errors, the tool and system vibrational behavior and the specific material.

However, it is difficult to obtain a comprehensive view of the system dynamics by analyzing a narrow measured surface topography area. A wider areal analysis may reflect some behavioral changes on surface 3D topography.

The next step of this research will be to check the developed mathematical model with different milling machines, with different alignment errors and vibrational behavior. The model may then be adjusted to be applicable for other surface topography parameters related with Standard ISO 25178:2012.

ACKNOWLEDGMENTS

This research has been conducted through scientific collaboration between Universitat Politècnica de València (Valencia, Spain), Riga Technical University (Riga, Latvia) and Tallinn University of Technology (Tallinn, Estonia).

REFERENCES

[1] T.S. Babin, J.M. Lee, J.W. Sutherland, S.G. Kapoor, "A model for end milled surface topography", Manufacturing Engineering Transactions, SME, North American Manufacturing Research Inst, ISBN - 0872631869, pgs. 362-368, 1985;

[2] J. Sutherland and R. DeVor, "A dynamic model of the cutting force system in the end milling process," *Sensors and Controls for Manufacturing*, vol. PED-33, pp. 53–62, 1987;

[3] J.W. Sutherland, T.S. Babin, "The geometry of surfaces generated by the bottom of an end mill", Sensors and Controls for Mechanics, ASME PED, Vol. 33, pp. 53-62, 1988

[4] I. Buj-Corral, J. Vivancos-Calvet, and H. González-Rojas, "Influence of feed, eccentricity and helix angle on topography obtained in side milling processes," *Int. J. Mach. Tools Manuf.*, vol. 51, no. 12, pp. 889–897, 2011;

[5] I. Buj-Corral, J. Vivancos-Calvet, and A. Domínguez-Fernández, "Surface topography in ball-end milling processes as a function of feed per tooth and radial depth of cut," *Int. J. Mach. Tools Manuf.*, vol. 53, no. 1, pp. 151–159, 2012;

[6] M. Arizmendi *et al.*, "Model development for the prediction of surface topography generated by ball-end mills taking into account the tool parallel axis offset. Experimental validation," *CIRP Ann. - Manuf. Technol.*, vol. 57, no. 1, pp. 101–104, 2008;

[7] Y. Altintaş and E. Budak, "Analytical Prediction of Stability Lobes in Milling," *CIRP Ann. - Manuf. Technol.*, vol. 44, no. 1, pp. 357–362, 1995;

[8] E. BUDAK, "Mechanics and dynamics of milling thin walled structures," p. 284, 1994.

[9] D. Kyun Baek, T. Jo Ko, and H. Sool Kim, "A dynamic surface roughness model for face milling," *Precis. Eng.*, vol. 20, no. 97, pp. 171–178, 1997;

[10] H. Moradi, G. Vossoughi, M. R. Movahhedy, and M. T. Ahmadian, "Forced vibration analysis of the milling process with structural nonlinearity, internal resonance, tool wear and process damping effects," *Int. J. Non. Linear. Mech.*, vol. 54, pp. 22–34, 2013;

[11] A. Weremczuk, R. Rusinek, and J. Warminski, "The Concept of Active Elimination of Vibrations in Milling Process," *Procedia CIRP*, vol. 31, pp. 82–87, 2015;

[12] S. Wojciechowski, P. Twardowski, M. Pelic, R. W. Maruda, S. Barrans, and G. M. Krolczyk, "Precision surface characterization for finish cylindrical milling with dynamic tool displacements model," *Precis. Eng.*, vol. 46, pp. 158–165, 2016;

[13] A. Logins, P. Rosado Castellano, S. C. Gutiérrez Rubert, R. Torres, T. Torims, F. Sergejev, Influence of Tool Deformations and Mounting Inaccuracies on 3D Surface Topology, Proceedings of Thirteenth International Conference on High-Speed Machining, Metz, France 2016;

[14] ISO 25178-2:2012, Geometrical product specifications (GPS) - Surface texture: Areal - Part 2: Terms, definitions and surface texture parameters, http://www.iso.org/iso/catalogue_detail.htm?csnumber=42785, 2012.

https://doi.org/10.1115/IMECE2017-72636
ISBN: 978-0-7918-5835-6